

## TECHNICAL PROGRESS REPORT

# **Progress Report on Effect of Bicarbonate on the Autunite Dissolution in the Presence of *Shewanella oneidensis* MR-1 under Anaerobic Conditions**

**Date Submitted:**

February 15, 2016

**Principal Investigator:**

Leonel E. Lagos, Ph.D., PMP®

**FIU Applied Research Center Collaborators:**

Yelena Katsenovich, Ph.D.

Vasileios Anagnostopoulos, Ph.D.

Sandra Herrera, Graduate Research Assistant

**PNNL Collaborator:**

Brady Lee, Ph.D.

Hope Lee, Ph.D.

**Prepared for:**

U.S. Department of Energy

Office of Environmental Management

Under Cooperative Agreement No. DE-EM0000598



**Applied Research Center**  
FLORIDA INTERNATIONAL UNIVERSITY

#### **DISCLAIMER**

This report was prepared as an account of work sponsored by an agency of the United States government. Neither the United States government nor any agency thereof, nor any of their employees, nor any of its contractors, subcontractors, nor their employees makes any warranty, express or implied, or assumes any legal liability or responsibility for the accuracy, completeness, or usefulness of any information, apparatus, product, or process disclosed, or represents that its use would not infringe upon privately owned rights. Reference herein to any specific commercial product, process, or service by trade name, trademark, manufacturer, or otherwise does not necessarily constitute or imply its endorsement, recommendation, or favoring by the United States government or any other agency thereof. The views and opinions of authors expressed herein do not necessarily state or reflect those of the United States government or any agency thereof.

## Table of Contents

Table of Figures .....	iv
List of Tables .....	v
Introduction .....	1
Objectives .....	2
Materials and Methods.....	2
3.1 Bicarbonate media solution preparation.....	2
3.2 <i>Shewanella oneidensis</i> MR-1 growth conditions.....	2
3.3 Autunite biodissolution experiments .....	3
3.4 Protein analysis .....	4
3.5 Sampling and elemental analysis.....	5
3.6 SEM-EDS analysis .....	6
Results and Discussion .....	6
4.1 Elemental analysis .....	6
4.2 Cell density and cell viability per plates.....	12
4.3 pH monitoring and protein analysis .....	14
4.4 SEM-EDS analysis and speciation studies .....	17
Future Work.....	20
Acknowledgement .....	20
References .....	20

## Table of Figures

Figure 1. 20-mL glass scintillation vial prepared with media amended with $\text{KHCO}_3$ and autunite mineral.	4
Figure 2. Sampling schedule before and after inoculation .....	4
Figure 3. Sacrificial vials inside the anaerobic glove box, prepared to conduct the autunite biodissolution experiment.....	4
Figure 4. Uranium concentration as a function of time for bicarbonate-free samples.....	6
Figure 5. Uranium concentration as a function of time for samples amended with 3 mM bicarbonate.....	7
Figure 6. Uranium concentration as a function of time for samples amended with 10 mM bicarbonate...	8
Figure 7. Uranium concentration in the aqueous phase in the presence of <i>Shewanella oneidensis</i> as a function of time, for three different bicarbonate conditions.....	8
Figure 8. Calcium concentration as a function of time for bicarbonate-free samples. Red points represent biotic samples while blue points represent abiotic samples. ....	9
Figure 9. Calcium concentration as a function of time for samples amended with 3 mM bicarbonate. Red points represent biotic samples while blue points represent abiotic samples. ....	9
Figure 10. Calcium concentration as a function of time for samples amended with 10 mM bicarbonate. Red points represent biotic samples while blue points represent abiotic samples. ....	10
Figure 11. Phosphorous concentration as a function of time for bicarbonate-free samples. Red points represent biotic samples while blue points represent abiotic samples. ....	11
Figure 12. Phosphorous concentration as a function of time for samples amended with 3 mM bicarbonate. Red points represent biotic samples while blue points represent abiotic samples.....	11
Figure 13. Phosphorous concentration as a function of time for samples amended with 10 mM bicarbonate. Red points represent biotic samples while blue points represent abiotic samples.....	12
Figure 14. Changes in the direct cells counting for samples containing varying concentrations of bicarbonate .....	13
Figure 15. Results for the total cells density versus viable cells for a) 0 mM $\text{HCO}_3^-$ ; b) 3 mM $\text{HCO}_3^-$ ; c) 10 mM $\text{HCO}_3^-$ .....	13
Figure 16. pH of autunite suspensions as a function of time. Red lines represent biotic samples and blue lines abiotic samples.....	14
Figure 17. Protein concentration as a function of time for <i>Shewanella oneidensis</i> grown under anaerobic conditions.....	15
Figure 18. Correlation between cell density of <i>Shewanella oneidensis</i> MR1 and protein content.....	16
Figure 19. The variation of cell density (logarithmic scale) as function of time .....	16
Figure 20. SEM image revealing structural damage of autunite and associated elemental composition by EDS analysis.....	17

Figure 21. Bacterial activity on the surface of autunite..... 18

Figure 22. Secondary mineral particles coating on the surface of autunite and EDS analysis ..... 18

## List of Tables

Table 1. Soluble and Saturated Species for All Three Conditons Studied (bicarbonate-free samples and samples amended with 3 and 10 mM bicarbonate)..... 19

## Introduction

Uranium is a key soil and groundwater contaminant at many U.S. Department of Energy sites, serving a leading role in the nation's defense for over 50 years. Uranium contamination of soil and groundwater is of great environmental concern due to the toxicological properties of the uranyl species. The behavior of uranium and its mobility in the subsurface is affected by various factors such as porewater and groundwater chemical composition, soil mineralogy, and microorganisms that thrive under these conditions. Uranium exists in four oxidation states but, under oxidizing conditions, it dominates as a highly soluble and stable uranyl ion,  $\text{UO}_2^{2+}$ . In neutral or basic pH conditions, uranium undergoes hydrolysis in aqueous solutions and can readily complex with a wide variety of ligands such as carbonate, nitrate and phosphate. In a bicarbonate-rich environment, carbonate anions are an important complexing agent for U(VI), and soluble uranyl-carbonate complexes are formed, such as negatively charged  $\text{UO}_2(\text{CO}_3)_2^{2-}$  and  $\text{UO}_2(\text{CO}_3)_3^{4-}$ , as well as neutral complexes such as  $\text{UO}_2\text{CO}_3$  (Bachmaf et al., 2008). The presence of carbonates clearly affects the dissolution of actinides and facilitates uranium desorption reactions from soil and sediments, thus increasing uranium mobility in natural waters (Langmuir, 1978). The above mentioned complexes have been identified in contaminated pore water at the Hanford Site, Washington State, and have been shown to inhibit the microbial reduction of U(VI) (Bernhard et al., 2001; Brooks et al., 2003).

The addition of tripolyphosphate amendments is one of the methods used to decrease the concentration of soluble uranium in contaminated plumes. The introduction of sodium tripolyphosphate into uranium-bearing saturated porous media results in the formation of uranyl phosphate solid phases (autunite) of general formula  $\{X_{1-2}[(\text{UO}_2)(\text{PO}_4)]_2 \cdot 1 \cdot n\text{H}_2\text{O}\}$ , where X is a monovalent or divalent cation. The stability of the uranyl phosphate solids in the subsurface is a critical factor that allows for determining the long-term effectiveness of the sodium tripolyphosphate remediation strategy. The presence of soil bacteria can affect uranium mobility significantly. Bacteria, in an effort to obtain phosphorous, a vital nutrient for their metabolism, may dissolve uranyl-phosphate minerals, thus liberating uranium in the aqueous phase. In addition to the biological activity, the presence of bicarbonate ions seems to enhance the release of U(VI) into the aqueous phase (Gudavalli et al., 2013). Natural systems are complex and their behavior is dictated by the synergistic and/or antagonistic effect of both biotic and physicochemical factors.

The Columbia River, adjacent to the Hanford Site, exhibits large stage variations, causing fluctuations in the water table. These water table fluctuations and multiple rise-and-fall cycles in the river created an oxic-anoxic interface in this region. Previous assessments of Hanford sediment samples collected from this area noted a decline in cultivable aerobic bacteria and suggested the presence of facultative anaerobic bacteria (Lin et al., 2012; Marshall et al., 2008). Therefore, understanding the role of facultative and anaerobic bacteria (e.g., *Shewanella*) as

one of the factors affecting the stability of autunite solids is very important for designing a successful environmental remediation strategy.

## Objectives

The objective of this research is to investigate autunite dissolution under anaerobic conditions by focusing on the bacterial strains of *Shewanella oneidensis* MR1 sp. There have been a few studies on the microbial dissolution of autunite in the anaerobic conditions examining dissimilatory metal-reducing bacteria (DMRB) (*Shewanella putrefaciens* 200R) (Smeaton et al., 2008) and *Shewanella oneidensis* MR1 (Sheng & Fein, 2013; Sheng & Fein, 2014b). Previous experiments with aerobic *Arthrobacter oxydans* strains illustrated a bio-enhanced release of U(VI) from natural Ca-autunite in the presence of various concentrations of bicarbonate. *Arthrobacter* strains, G968 and G975, which exhibited various degrees of tolerance to U(VI) toxicity, were able to bio-enhance the release of U(VI) from natural Ca-autunite at almost the same capacity (Katsenovich et al., 2013). Previous research by Bencheikh-Latmani and Leckie (Bencheikh-Latmani & Leckie, 2003) and Katsenovich (Katsenovich et al., 2012) has also suggested that uranyl-carbonate complexes formed in the solution do not strongly interact with the negatively charged bacterial surface, which in turn can mitigate U(VI) toxicity on cells.

## Materials and Methods

### 3.1 Bicarbonate media solution preparation

The media solution was prepared in 1 L of DIW buffered with 0.02 M Na-Hepes buffer with pH adjusted to 7.1 with 0.1 mol/L HCl or NaOH. Sodium lactate ( $C_3H_5NaO_3$ , 60% w/w) was added to the solution with a concentration of 0.024 mol/L. The solution was divided into three bottles and sterilized by autoclaving at 121°C, 15 psi for 15 min and cooled at room temperature. As the experiment is based on the investigation of bacteria interactions in the presence of different bicarbonate concentrations, potassium bicarbonate salt was added to the autoclaved bottles to obtain 3 mM and 10 mM bicarbonate; the remaining bottle was kept bicarbonate-free. This accounts for a total of three concentrations of bicarbonate for the experiment tested. Next, the solutions were filter-sterilized and the sterile bottles were stored in the anaerobic chamber until the beginning of the experiment.

### 3.2 *Shewanella oneidensis* MR-1 growth conditions

*Shewanella oneidensis* MR1 strains were obtained from the Pacific Northwest National Laboratory (PNNL) and stored at -80°C in 25% glycerol prior to use. A starter culture was grown on sterile hard and liquid Luria-Bertani (LB) media prepared with 10.0 g of tryptone, 5.0 g of yeast extract, and 10.0 g of sodium chloride, with a pH of 7.0. Hard media required an addition of 15.0 g of agar. A fresh culture was grown in 15-mL tubes placed in the incubator at 30°C while being shaken at 100 rpm (C24KC refrigerated incubator shaker; New Brunswick Scientific).

Bacterial cells were grown overnight in an LB liquid medium and then harvested for the cell density (cells/mL) calculations using a glass hemocytometer (Fisher Scientific, Pittsburg, PA) or INCYTO C-Chip disposable hemocytometer (SKC America). Once the average cell count was obtained, it was multiplied by the dilution factor and the volume factor ( $10^4$ ) in order to calculate the final concentration of cells per mL. The number of cells/mL in the stock suspension was used to estimate a desired volume (mL) of a bacterial suspension needed for the inoculation of each bottle. To account for viable bacteria, a well-mixed homogeneous aliquot (0.01 mL - 0.1 mL) of the suspension from each test vial was uniformly spread on the sterile Petri dishes containing a LB growth media mixed with 15 g/L of agar. Inoculated plates were kept inverted in an incubator at 30°C. Viable microorganisms were calculated from the number of colony-forming units (CFU) found on a specific dilution.

### **3.3 Autunite biodissolution experiments**

The autunite biodissolution experiments were performed by using 20-mL sacrificial glass scintillation vials as opposed to our past experiments where sampling was periodically conducted from the same 100-mL sealed bottle containing 50 mL of sterile medium. The sacrificial vials approach was chosen to avoid microbial cross- contamination during sampling events. Each vial was filled with 18 mg of autunite powder to provide a final U(VI) concentration of 4.4 mmol/L (Figure 1), which is similar to concentrations previously used in the mixed bioreactors. All prepared glass vials with autunite were covered with plastic caps and autoclaved for 15 min at 121°C to ensure sterile conditions. Each vial was amended with 10 mL of sterile media solution containing 0, 3, and 10 mM  $\text{KHCO}_3$ . After autunite equilibration, the samples were inoculated with the desired volume of bacterial suspension to obtain an initial cell density of  $10^6$  cells/mL. In addition, abiotic control vials were kept for each bicarbonate concentration and sampled in parallel with the experimental vials. Each set, prepared using a specific bicarbonate concentration, includes duplicate sacrificial biotic vials and an abiotic control. Samples were sacrificed at specific time intervals according to the sampling schedule. In addition, to allow the media solutions to equilibrate with the autunite, three abiotic samples were prepared at each bicarbonate concentration and sampled every 5 days before bacteria inoculation. The interval of time between sampling events after the media equilibrated with the autunite and bacteria inoculation was about 4-5 days, as shown in Figure 2. The total number of sacrificial vials for the duration of the experiment was calculated as 99.



**Figure 1.** 20-mL glass scintillation vial prepared with media amended with  $\text{KHCO}_3$  and autunite mineral.

inoculation															
Sampling	Day 3	Day 3	Day 7	Day 7	Day 10	Day 10	Day 10	Day 14	Day 14	Day 17	Day 17	Day 21	Day 21	Day 25	Day 25
Abiotic	0mM	3mM	0mM	3mM	0mM	3mM	0mM	0mM	3mM	0mM	3mM	0mM	3mM	0mM	3mM
Biotic	Duplicates							0mM	3mM	0mM	3mM	0mM	3mM	0mM	3mM
# vials	1	1	1	1	1	1	1	3	3	3	3	3	3	3	3
Legend															
0mM															
3mM															
10mM															
															Tot
															99

**Figure 2.** Sampling schedule before and after inoculation.

Experimental vials and bottles with the media solutions amended with bicarbonate were kept in an anaerobic chamber for the entire duration of the experiment (Figure 3).



**Figure 3.** Sacrificial vials inside the anaerobic glove box, prepared to conduct the autunite biodissolution experiment.

### 3.4 Protein analysis

For cell protein determination, a BCA (Pierce) protein analysis kit was used. For the preliminary assessment, a calibration curve was built using albumin as a standard solution and the absorbance was measured at 562 nm spectrophotometrically. The BCA protein assay is based on the highly selective colorimetric detection of the cuprous cation ( $\text{Cu}^+$ ) by bichinchonic acid (BCA) as a result of the reduction of  $\text{Cu}^{2+}$  to  $\text{Cu}^+$  by protein in an alkaline medium. A fresh

culture of facultative anaerobic bacteria *Shewanella oneidensis* MR1 was grown in two 15-mL tubes filled with LB liquid media to determine the relationship between the protein content and cell density. The tubes were placed in the incubator for two days at 30°C. After two days, the tubes were centrifuged and the pellet was washed with deionized water and re-suspended in 1.5 mL of DIW. The washing procedures were repeated twice. After washing, the cells were counted via hemocytometer and 1.2 mL from each vial was extracted into the 1.5-mL microcentrifuge tubes to be used for the bicinchoninic acid protein assay. The stock cell density concentrations in vial #1 and vial #2 were calculated as 884,210,526 cells/mL and 877,419,355 cells/mL, respectively. Following the protocol procedures, the cells were lysed by boiling at 100°C for 10 min and then cooled on ice. The addition of an alkaline medium followed and the samples were placed in a water bath (60°C) for 30 minutes. Several aliquots were taken from the stock cell solutions and a calibration curve was prepared by using albumin as a standard for the protein content and the absorbance was measured at 562 nm spectrophotometrically. Testing of this protocol yielded a detection limit of  $10^{5.9}$  cell/mL.

### 3.5 Sampling and elemental analysis

Prior to any further manipulation, the pH of the samples was recorded. Then, 1-mL aliquots were isolated from each vial and stored in the laboratory refrigerator for further uranium analysis by the kinetic phosphorescence analysis (KPA-11, Chemchek Instruments Inc.) instrument. The presence of organic content in the solutions can interfere with KPA measurements; hence, samples collected during the experiments were pre-processed by wet ashing followed by dry ashing procedures. A modified ashing technique described by Ejnik (Ejnik et al., 2000) was used for wet and dry ashing. Wet digestion was performed by the addition of 500  $\mu$ L of concentrated nitric acid ( $\text{HNO}_3$ ) and 500  $\mu$ L of concentrated hydrogen peroxide ( $\text{H}_2\text{O}_2$ ) to each vial; the vials were placed on a heating plate until full evaporation was achieved and a white solid residue was acquired. Occasionally, some samples turned yellow while ashing; 0.5 mL of peroxide was added to these samples and the process was continued until a white precipitate was obtained. The dry samples were placed in a furnace preheated to 450°C for 15 min and then allowed to cool at room temperature. Finally, precipitates obtained in the drying step were dissolved in 1 mL of 2 mol/L nitric acid and analyzed by means of the KPA instrument to determine uranium concentrations released into the aqueous phase as a function of time. In addition, calcium and phosphorous were determined by means of inductively coupled plasma – optical emission spectroscopy (ICP-OES 7300 Optima, Perkin Elmer) using calcium and phosphorous standards (Spex CertiPrep). ANOVA statistics were used to examine the results on the release of U(VI) due to varying concentrations of bicarbonate ions. The significance level was set at  $\alpha = 0.05$ . The results from elemental analysis were used in speciation modeling calculations by means of Visual Minteq and Hydra speciation software.

### 3.6 SEM-EDS analysis

The autunite samples, after isolation of aliquots for chemical analysis and protein analysis, were prepared for SEM-EDS analysis. Cells attached on autunite were first treated with 4 ml of 2% glutaraldehyde in 0.1 M HEPES at 4°C for 2h. Samples were then centrifuged, supernatant was decanted and the material was washed with 4 ml of 0.05 M HEPES for 10 min. After discarding the supernatant, the material was “dehydrated” in 4 consecutive steps: treatment with 35%, 70%, 90% and 100% of ethanol for 10 min at room temperature. Finally, a small quantity of hexamethyldisilazane (HMDS) (Pierce Biotechnology, Inc, obtained from Fisher Scientific) was introduced two times and the material was left to air-dry at room temperature for 10 min before being stored in a desiccator until SEM-EDS analysis (Braet et al., 1997; Hazrin-Chong & Manefield, 2012).

## Results and Discussion

### 4.1 Elemental analysis

Figure 4, Figure 5, and Figure 6 present concentrations of uranium measured by means of KPA in bicarbonate-free samples and samples amended with 3 mM and 10 mM of bicarbonate, respectively.

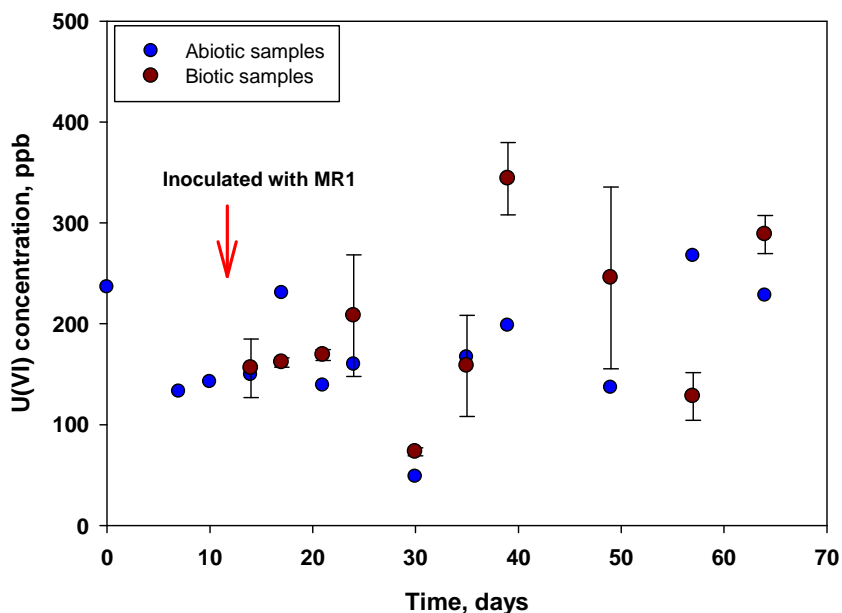


Figure 4. Uranium concentration as a function of time for bicarbonate-free samples.

In the case of bicarbonate-free samples, the amount of uranium released in the aqueous phase didn't show any statistically significant difference between abiotic and biotic samples (confidence level 95%,  $p=0.468$ ), denoting that the presence of *Shewanella oneidensis* does

not contribute to the release of uranium in the aqueous phase (Figure 4). It seems that the release of U(VI) in the aqueous phase is the outcome of the autunite mineral dissolution by the aqueous phase. Furthermore, no decrease in uranium was observed in the biotic samples after inoculation with *Shewanella oneidensis* (day 10), a fact that implies that there is no bioreduction of U(VI) to U(IV). On the other hand, in the samples amended with 3 and 10 mM bicarbonate, the inoculation with bacteria cells incurs a sharp increase in uranium concentration in the aqueous phase, most probably due to bacterial activity of dissolving autunite in order to obtain the metabolically necessary phosphorous. The steady state maximum concentrations of U(VI) detected were 3-6 fold higher compared to the corresponding bicarbonate-bearing abiotic controls at steady state. However, despite anaerobic conditions, no bioreduction of uranium was observed in the bicarbonate-amended samples and the concentration of uranium in the media solutions remained stable throughout the experiment (63 days) (Figure 5, Figure 6).

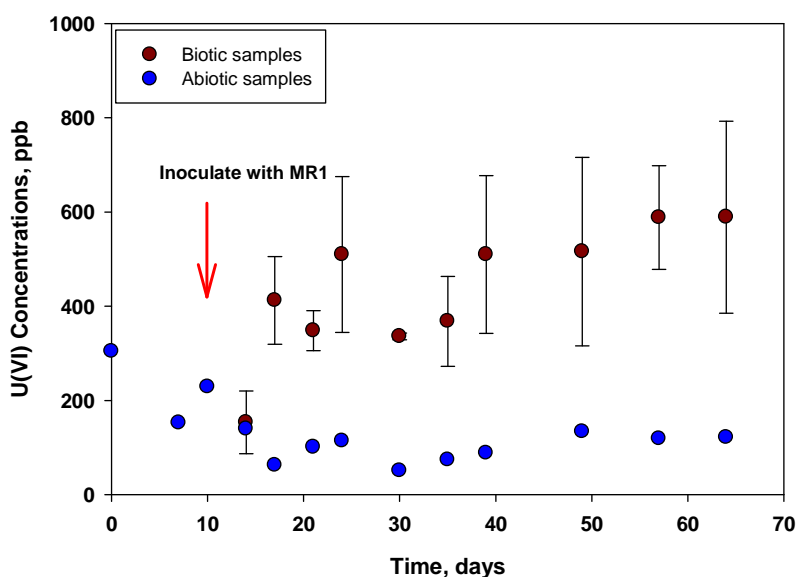


Figure 5. Uranium concentration as a function of time for samples amended with 3 mM bicarbonate.

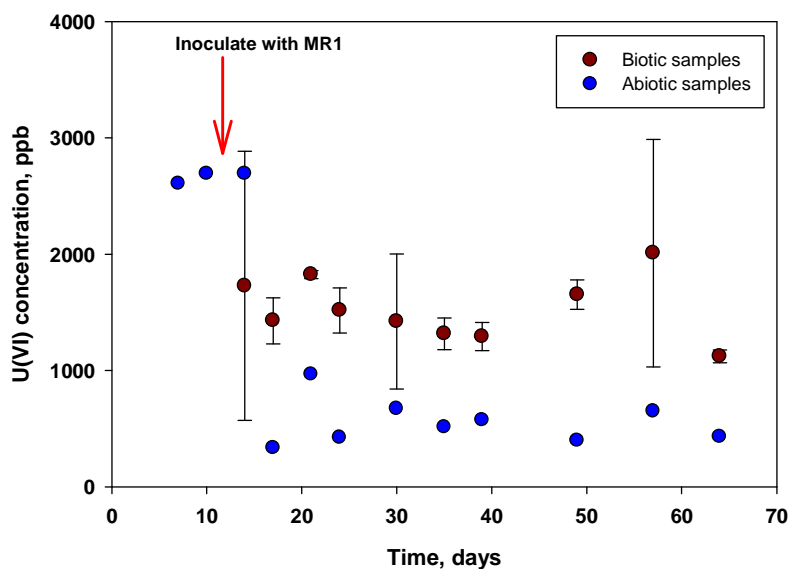


Figure 6. Uranium concentration as a function of time for samples amended with 10 mM bicarbonate.

Despite the fact that no bioreduction of U(VI) was observed in any of the conditions studied, the degree of uranium release among the different conditions in the presence of *Shewanella oneidensis* differed significantly (Figure 7). There was a progressive increase in uranium release as the concentration of bicarbonate in the sample increased ( $p=0.001$  among all groups for confidence intervals 95%).

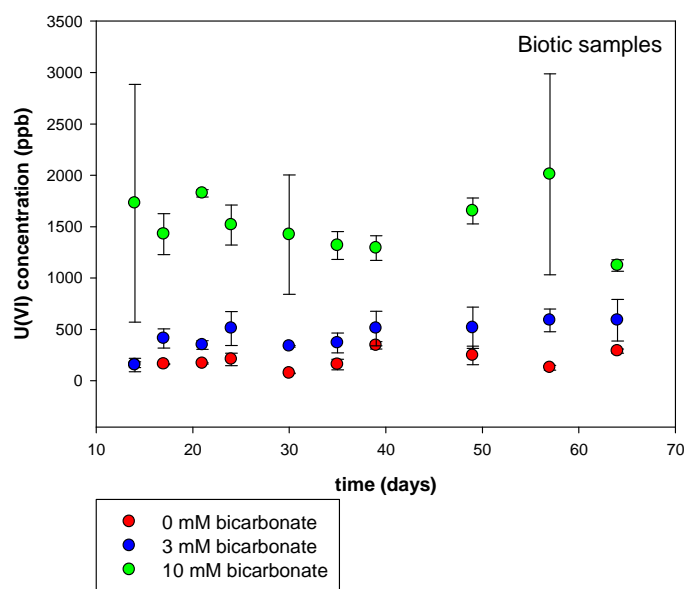
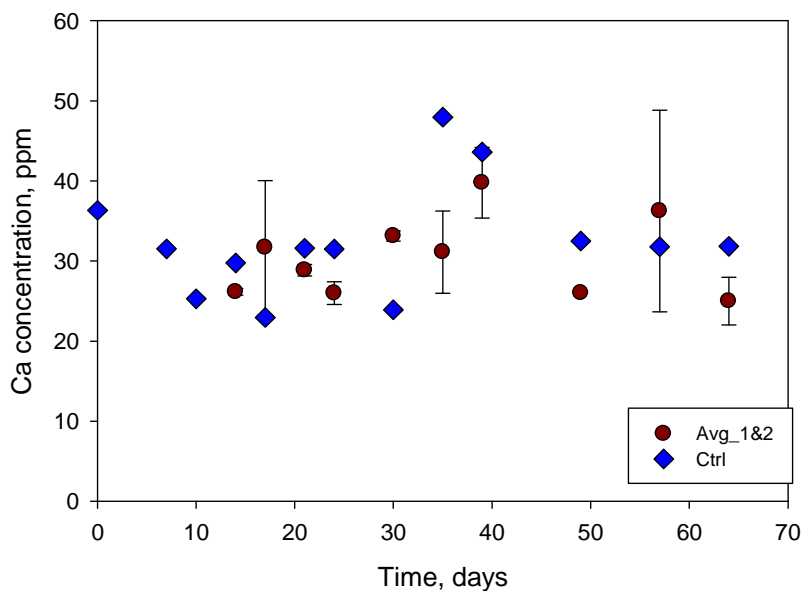
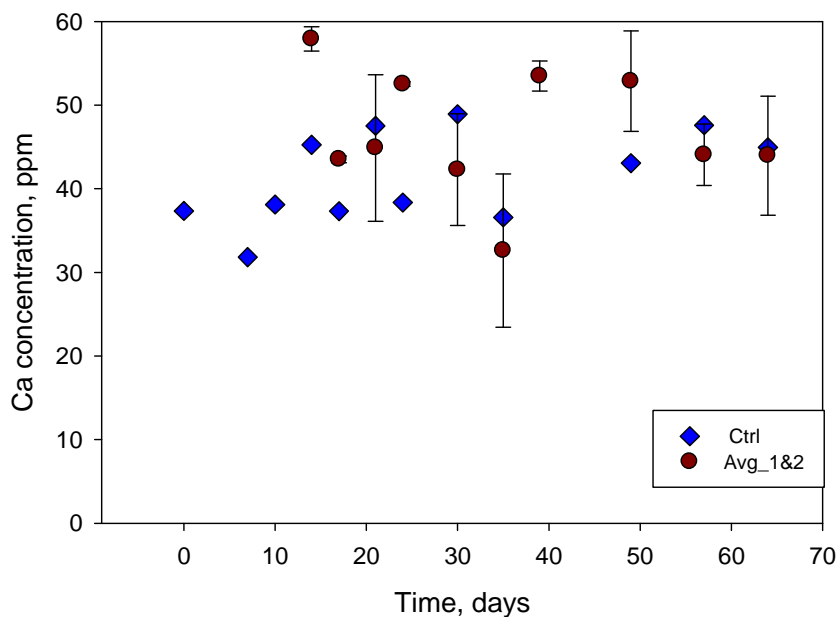


Figure 7. Uranium concentration in the aqueous phase in the presence of *Shewanella oneidensis* as a function of time, for three different bicarbonate conditions.

The dissolution of autunite also resulted in the release of calcium and phosphorous in the aqueous phase. The results for calcium analysis are presented in Figure 8- Figure 10.



**Figure 8. Calcium concentration as a function of time for bicarbonate-free samples. Red points represent biotic samples while blue points represent abiotic samples.**



**Figure 9. Calcium concentration as a function of time for samples amended with 3 mM bicarbonate. Red points represent biotic samples while blue points represent abiotic samples.**

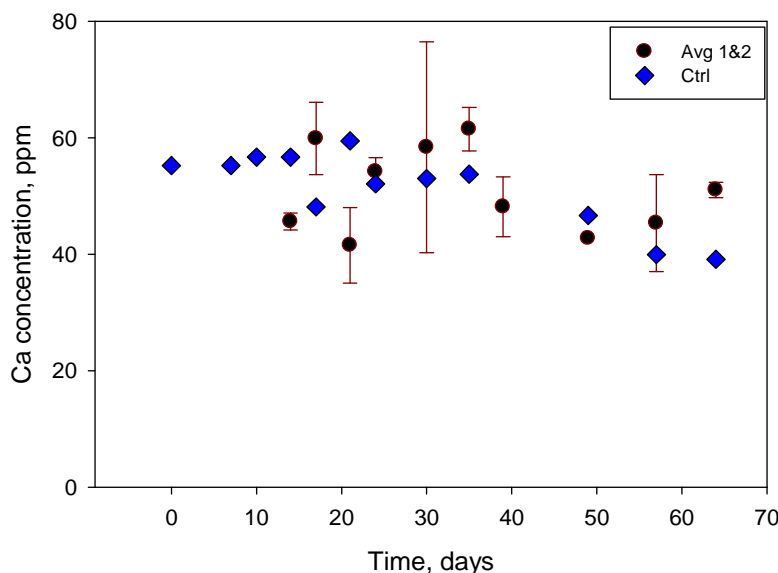


**Figure 10. Calcium concentration as a function of time for samples amended with 10 mM bicarbonate. Red points represent biotic samples while blue points represent abiotic samples.**

In bicarbonate-free samples, results revealed a similar trend between biotic and abiotic samples. Statistical evaluation suggested that there is not a significant difference between abiotic and biotic samples ( $p=0.476$ ). A similar trend was observed in the samples amended with 3 mM bicarbonate ( $p=0.965$ ) and with 10 mM bicarbonate ( $p=0.867$ , confidence interval 95%). In accordance with uranium results, higher concentrations of bicarbonate ions in the media solutions resulted in higher calcium release in the aqueous phase.

Despite of high variability of phosphorous concentrations between biotic duplicates, the results were similar to that tested for calcium: there was no significant difference between biotic and abiotic samples in all three categories ( $p=0.784$ ,  $p=0.793$  and  $p=0.644$  when comparing biotic and abiotic samples for bicarbonate-free, 3 mM and 10 mM amended samples, respectively, confidence interval 95%).

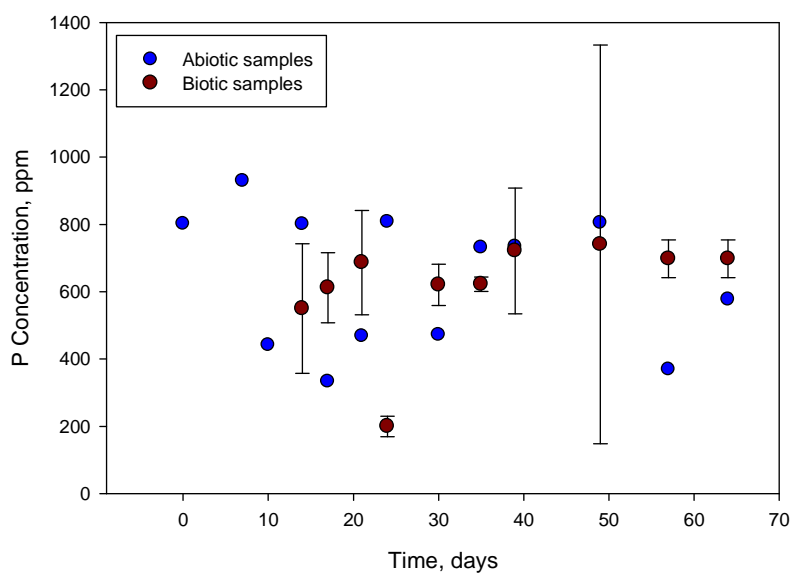


**Figure 11. Phosphorous concentration as a function of time for bicarbonate-free samples. Red points represent biotic samples while blue points represent abiotic samples.**

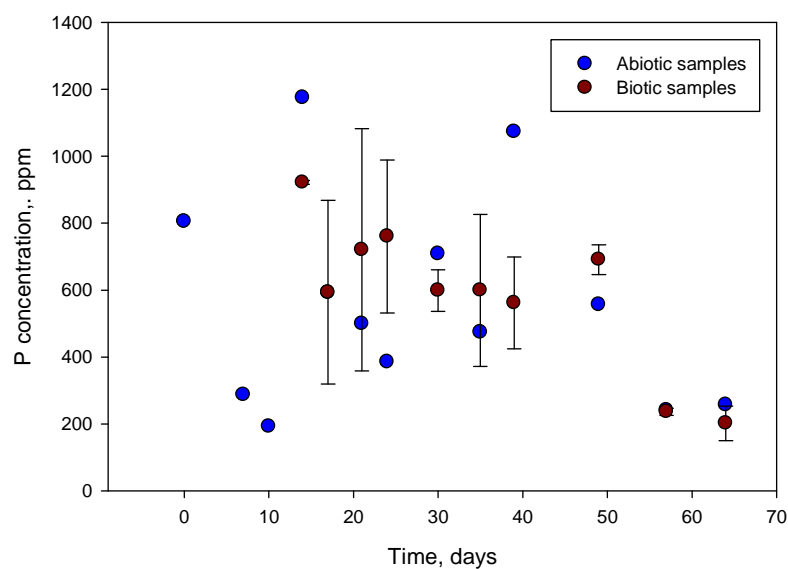


**Figure 12. Phosphorous concentration as a function of time for samples amended with 3 mM bicarbonate. Red points represent biotic samples while blue points represent abiotic samples.**

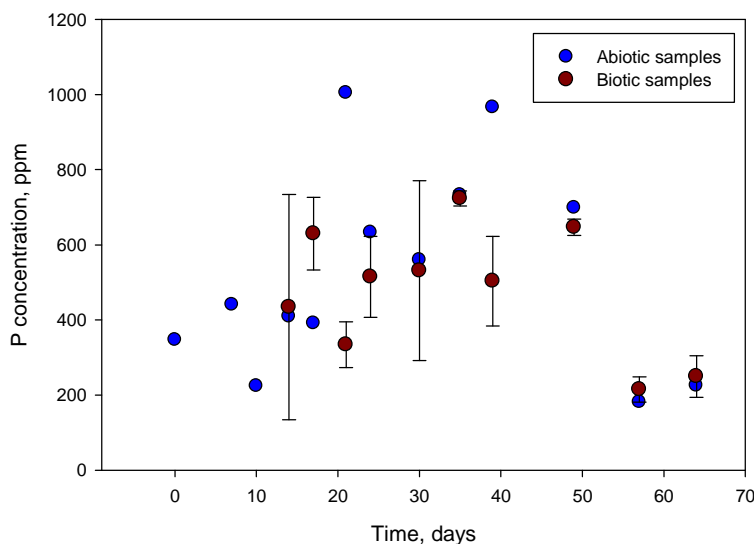


**Figure 13. Phosphorous concentration as a function of time for samples amended with 10 mM bicarbonate. Red points represent biotic samples while blue points represent abiotic samples.**

## 4.2 Cell density and cell viability per plates

Direct visual cell counting using a hemocytometer combined with a cell viability analysis using the spread plate method was conducted for each sampling event. The initial inoculation cell density was  $10^6$  cells/mL (log 6 cells/mL) for all biotic samples. In bicarbonate-free samples, cell densities for the duration of the experiment showed almost no change from the initial concentration (Figure 14). In contrast, samples amended with 3 mM and 10 mM of bicarbonate demonstrated almost 10-14 fold increases in cell density and values stabilized in the range of log 6.9- log 7.3 cell/mL by the end of experiment (Figure 14).

Cell viability, determined via counts of colony forming units (CFU/mL), was compared to the cell density obtained via direct cell counting. Samples containing 0 mM bicarbonate yielded on average about 11.1% of viable cells out of a total cell density that correlates to only  $1.1^5 \pm 1.0^5$  CFU/mL. In addition, viable cells showed a tendency to decrease with time. In samples amended with 3 mM and 10 mM of  $\text{HCO}_3$ , the ratio between viable cells and total cell density increased to 30-31%. Since the cell density in bicarbonate-amended solutions increased in average to  $1.0^7$ - $1.4^7$  cells/mL, the quantity of viable cells was determined to be on the order of  $2.2^6$ - $2.3^6$  CFU/mL, which is significantly higher than was observed in the bicarbonate-free solutions. The increase in total cell density and the quantity of viable cells might be an indication that the cells have acclimated to withstand uranium toxicity in the presence of bicarbonate ions. Figure 15 presents results for the total cell density versus viable cells for the three bicarbonate concentrations tested.

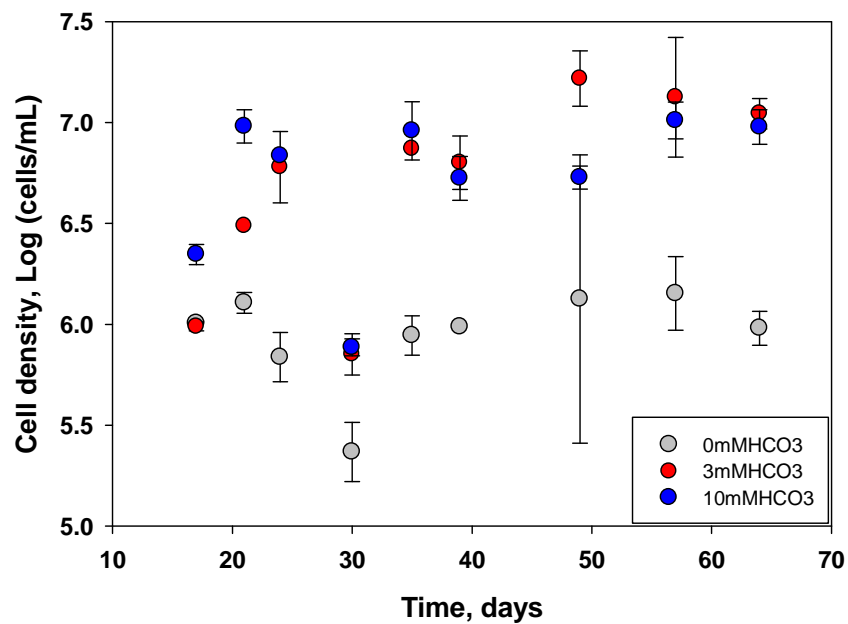


Figure 14. Changes in the direct cell counts for samples containing varying concentrations of bicarbonate.

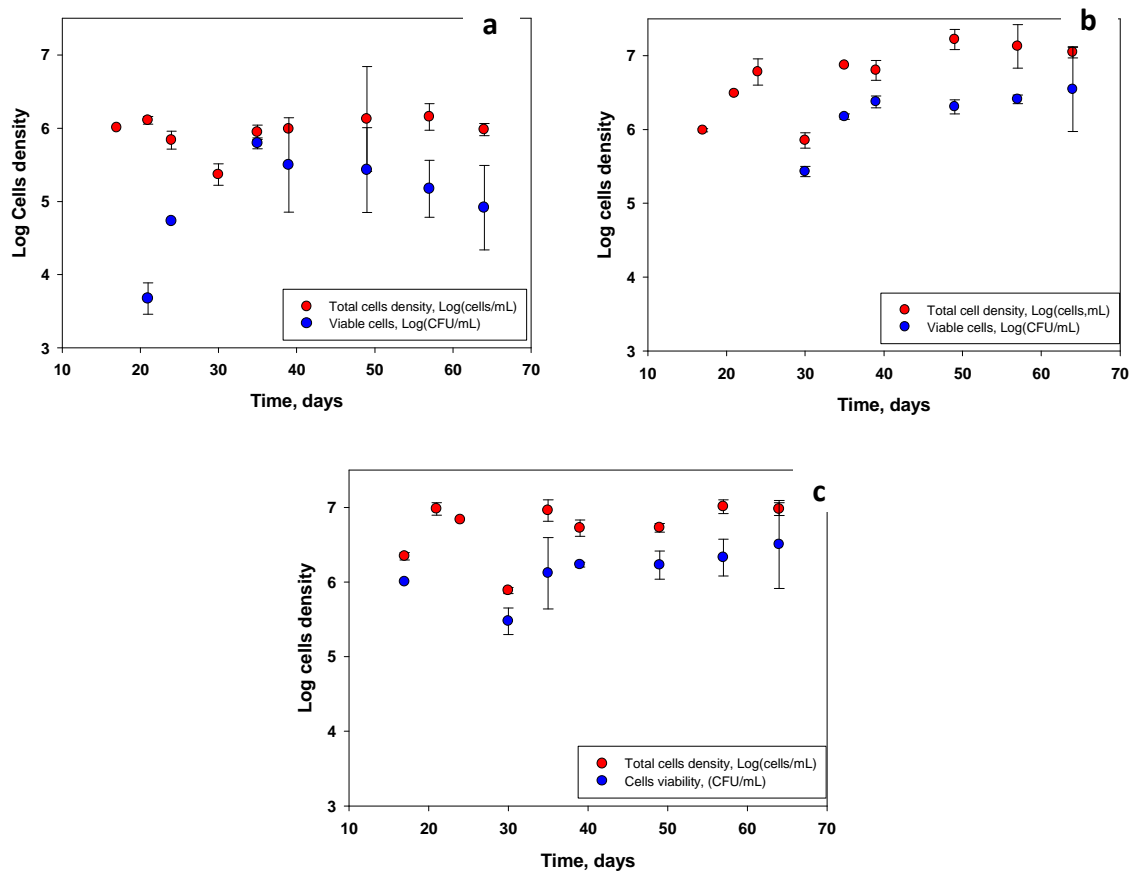


Figure 15. Results for the total cell density versus viable cells for a) 0 mM HCO<sub>3</sub><sup>-</sup>; b) 3 mM HCO<sub>3</sub><sup>-</sup>; c) 10 mM HCO<sub>3</sub><sup>-</sup>.

### 4.3 pH monitoring and protein analysis

pH monitoring was conducted for every sampling event. For all the samples, bicarbonate-free and the ones amended with 3 and 10 mM bicarbonate, an increase in pH (0.7 pH units) was observed at day 21. However, there was no similar trend observed for the control abiotic samples, where pH remained practically unchanged until the end of the experiment (Figure 16). Facultative anaerobic bacteria in the presence of a terminal electron donor ( $O_2$ ) can convert sugars to  $CO_2$  through respiration (Lin et al., 2005), whereas in the absence of a terminal electron donor, sugars can be converted into organic molecules through fermentation reactions (Sánchez et al., 2005). In the case of *Shewanella oneidensis* MR-1, the bacteria under aerobic conditions have been reported in literature to produce no other by products than  $CO_2$  (Pinchuk et al., 2011), which when dissolved in water forms carbonic acid, hence decreasing the pH. On the other hand, *Shewanella oneidensis* has been reported to metabolically excrete acetate and formate when grown on lactate as a sole carbon source under anaerobic conditions and the production of  $CO_2$  was very limited (Claessens et al., 2006; Meshulam-Simon et al., 2007; Pinchuk et al., 2011; Tang et al., 2006). Assuming that the release of  $CO_2$  is the determining factor for pH fluctuation, the limited release of  $CO_2$  scenario may be a possible explanation for the experimental results presented in Figure 16.

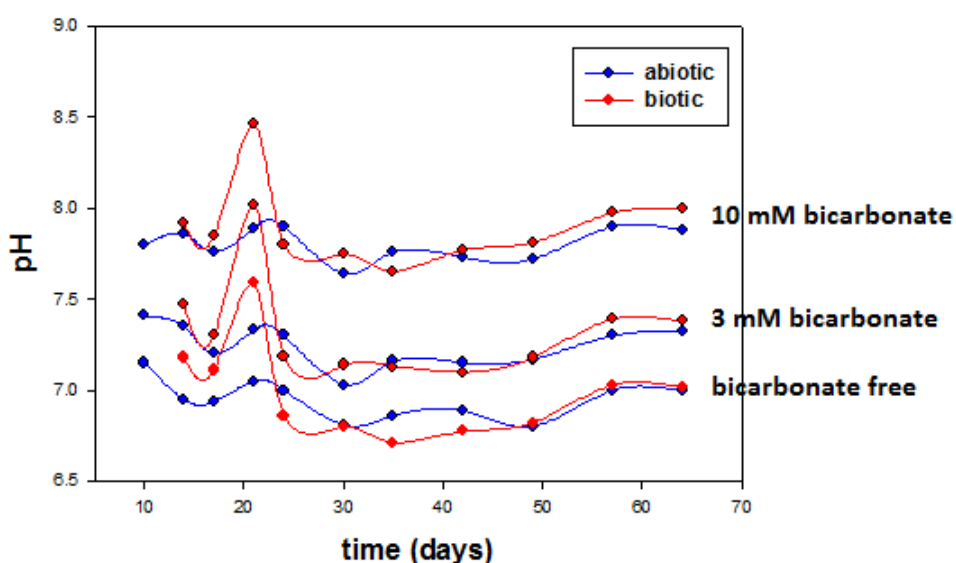


Figure 16. pH of autunite suspensions as a function of time. Red lines represent biotic samples and blue lines abiotic samples.

Interestingly, the protein analysis revealed a very similar trend with a sharp increase of protein content at day 21, and the increase was more profound in the samples amended with 3 and 10 mM bicarbonate (Figure 17). A correlation between cell density of fresh *Shewanella oneidensis* suspensions and protein content fits to a linear regression (Figure 18). Based on the estimated

regression function, the experimentally determined protein content was converted to the cell density for all bicarbonate concentrations tested (Figure 19). The correlation coefficient between the protein content and the calculated amount of cells present in the medium suggested an increase in cell growth at day 21. Cells cultivated in media amended with 10 mM  $\text{HCO}_3^-$  demonstrated almost 3 times higher density than that in bicarbonate-free solutions. This vigorous cell growth demonstrated through a sharp increase in protein concentration in the medium coincided with the pH increase. In the case of bicarbonate-free samples, the cell density reached  $10^{7.5}$  from  $10^6$  cells/ml, whereas in the case of samples amended with 3 mM and 10 mM bicarbonate, the change in cell density was much greater, from  $10^6$  cells/ml to  $10^{10}$  cells/mL.

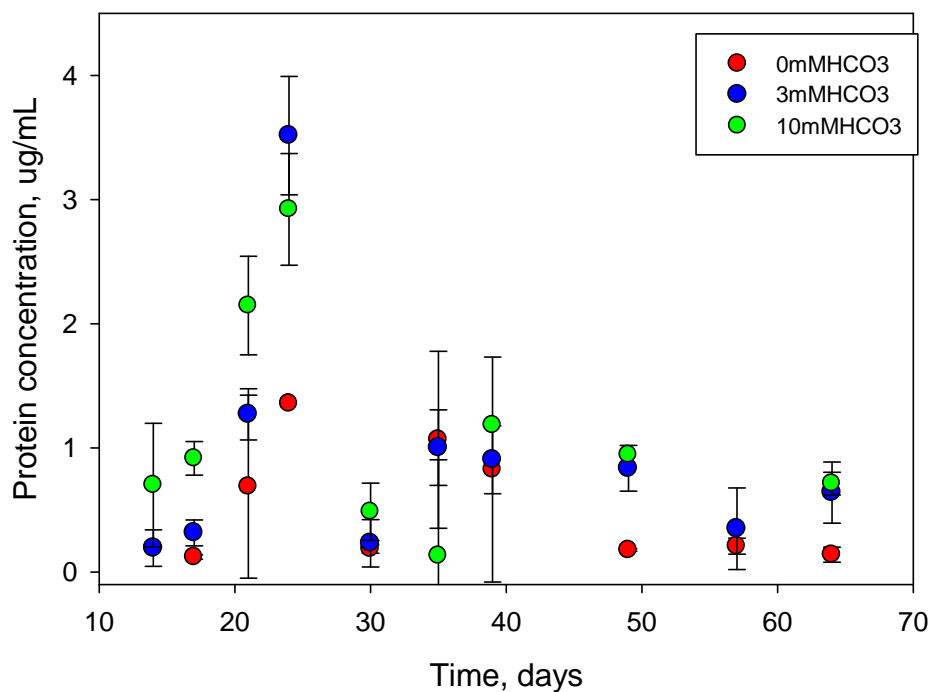


Figure 17. Protein concentration as a function of time for *Shewanella oneidensis* grown under anaerobic conditions.

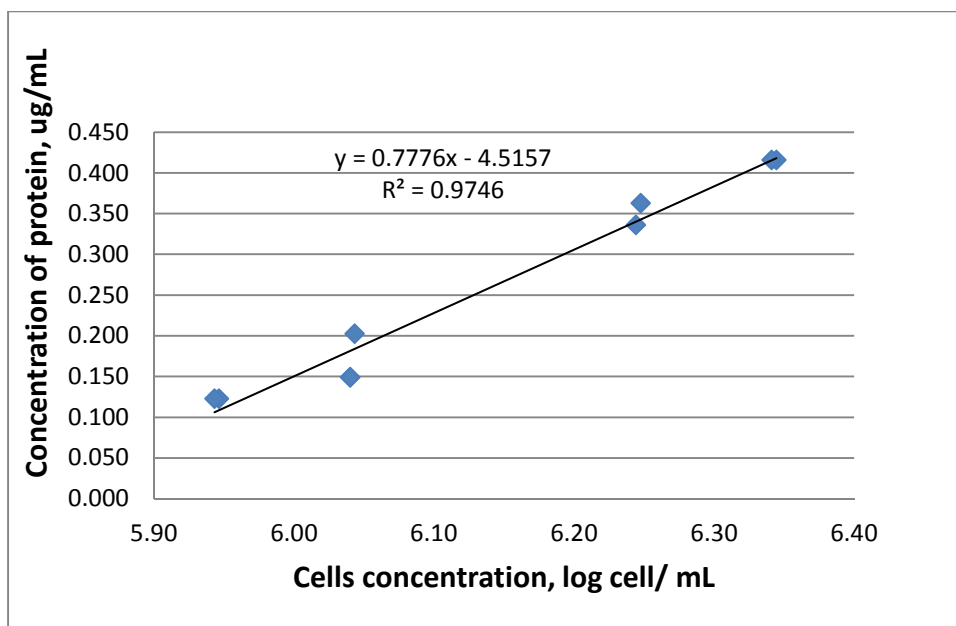


Figure 18. Correlation between cell density of *Shewanella oneidensis* MR1 and protein content.

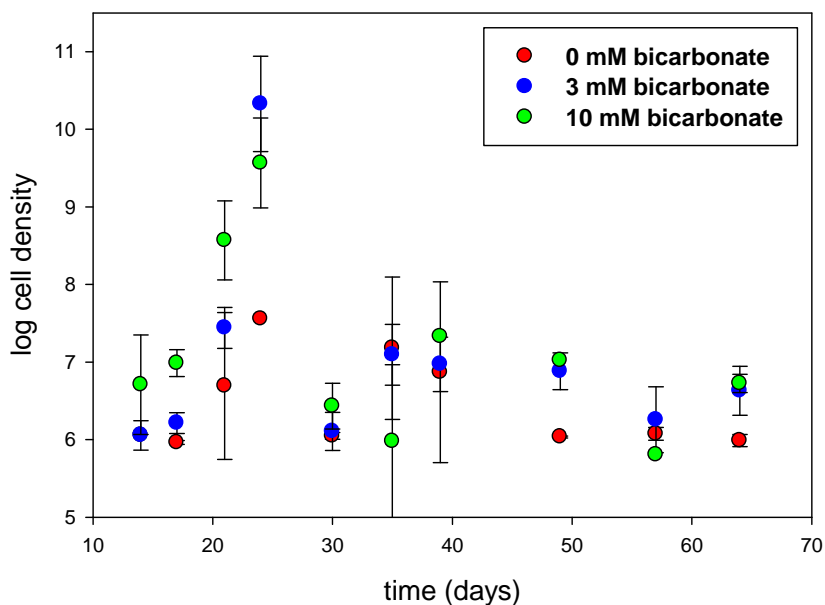


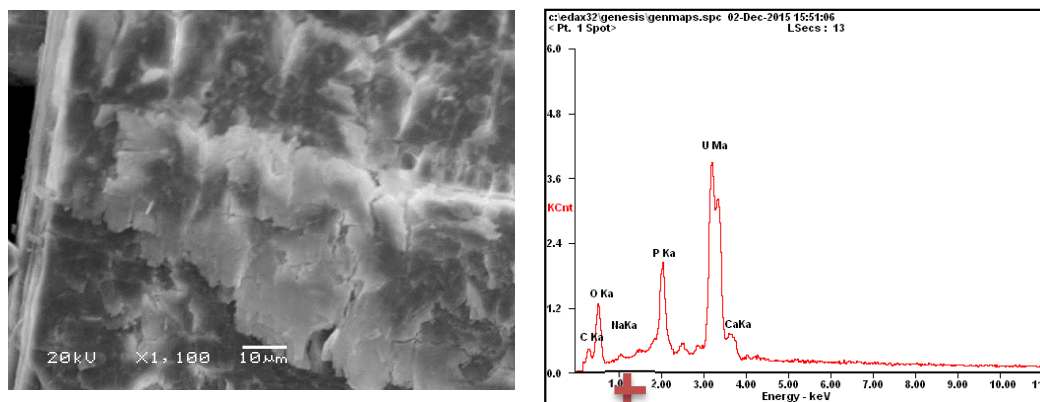
Figure 19. The variation of cell density (logarithmic scale) as function of time.

The theoretically calculated cell density values presented in Figure 19 correspond to the total cell density, which is a sum of both viable and non-viable cells. The nature of the protein determination protocol does not allow estimating the amount of viable and non-viable cells. Overall, the theoretically calculated total cell density looks overestimated compared to the direct visual cell density counting. This might be due to the fact that Figure 19 calculations were based on *Shewanella oneidensis* cells grown in the bacteria culture medium. There is a

possibility that exposure to uranium affected the cell physiology and protein content, which might have resulted in changes of protein masses (Khemiri et al., 2014). So, the correlation between cell density and protein content obtained for the control cells grown in culture media might not be valid for cells exposed to uranium. Further experiments on uranium-bacteria interactions conducted without autunite solids will help to investigate changes in protein content as a result of uranium exposure.

#### 4.4 SEM-EDS analysis and speciation studies

Images of autunite solids taken by means of SEM revealed the destruction of autunite as a consequence of bicarbonate effect and bacterial activity (Figure 20). In the bicarbonate-free samples, no bacteria were observed on the autunite surface. This finding may explain the fact that there was not any uranium release in the aqueous phase due to bacterial activity in the bicarbonate-free samples (**Error! Reference source not found.**). On the other hand, bacteria were clearly observed on the mineral's surface in the case of samples amended with 3 mM and 10 mM bicarbonate (Figure 21). Bacteria can attach on the mineral surfaces through specific structures called extracellular polymeric substances (EPS), comprised mostly of saccharides and proteins and secondarily DNA and lipids (Donlan, 2002). Nevertheless, no extensive (covering most of the surface or creating vertical multilayer formations) biofilm was observed in these samples. The formation of an extensive film has been reported to be crucial for metal reduction by *Shewanella* and is regulated by the presence of oxygen (McLean et al., 2008; Wu et al., 2013). Our experiments were performed in the absence of oxygen, hence the absence of an extensive biofilm, as well as bioreduction, may be justifiable.



Element	Wt%	At%
CK	01.43	07.80
OK	14.19	57.90
NaK	00.55	01.57
PK	04.28	09.03
CaK	01.39	02.26
UL	78.15	21.44
Matrix	Correction	ZAF

Figure 20. SEM image revealing structural damage of autunite and associated elemental composition by EDS analysis.

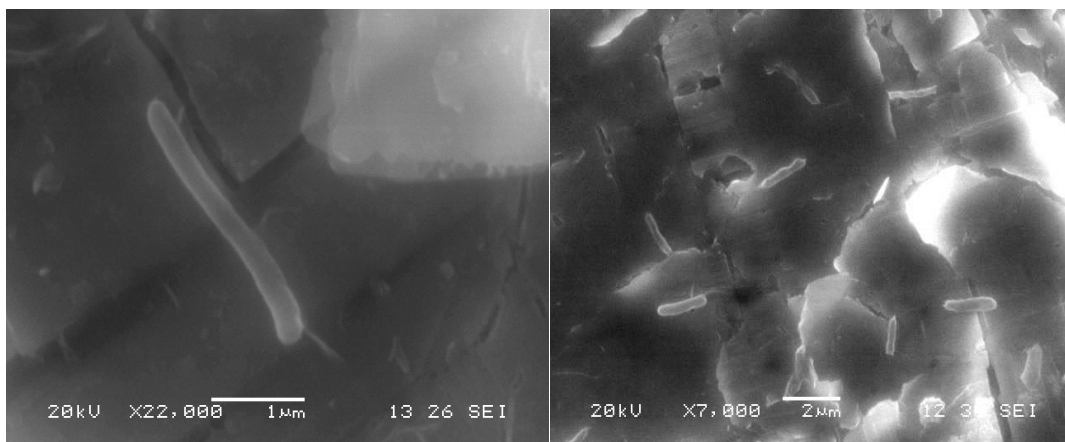
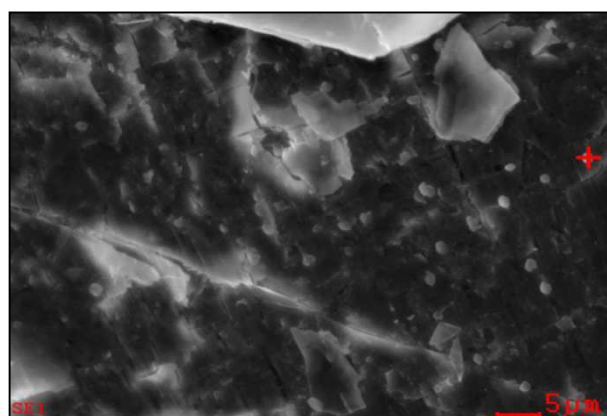


**Figure 21. Bacterial activity on the surface of autunite.**

A study by Thormann investigated the biofilm formation by *Shewanella* and reported the formation of a layer of biofilm initially until the coverage of the surface and, consequently, the formation of vertical towering biofilm structures (Thormann et al., 2004). Furthermore, acetate and lactate have been reported to be less effective stimulants for U(VI) reduction, whereas more complex organic electron donors have been directly correlated to the ability of DMRB to reduce U(VI) (Barlett, 2014).

The SEM photos also revealed the formation of secondary minerals, mainly uranyl phosphates and uranyl carbonates, coating the surface of autunite (Figure 22). These secondary minerals are a result of saturation of the aqueous phase due to the release uranium, calcium and phosphorous under the conditions studied.



Element	Wt%	At%
CK	06.22	14.63
NK	09.87	19.91
OK	28.16	49.76
NaK	00.65	00.80
PK	05.92	05.40
UM	42.96	05.10
CaK	06.23	04.39

**Figure 22. Secondary mineral particles coating on the surface of autunite and EDS analysis.**

The formation of the secondary minerals was predicted by the calculations performed by means of speciation softwares (Visual Minteq and Hydra). The soluble species were also predicted by the speciation softwares under the experimental conditions and the results are presented in Table 1. As can be seen, the saturation of hydroxylapatite (calcium phosphate mineral) and uranyl-phosphate minerals is predicted in all cases. Nevertheless, the elemental

analysis results did not reveal any decrease in any of these elements throughout the duration of the experiment; on the contrary, uranium, calcium and phosphorous seem to be unaffected. A decrease in the concentration of those elements could be associated with the formation of secondary minerals (and bioreduction, only in the case of uranium). A possible explanation could be that the rate of release of those elements in the aqueous phase is very similar to the rate of micro-precipitation of secondary minerals, which removes these elements from the aqueous phase; hence, the apparent concentration of those elements remains the same. Additional experiments, as outlined in the “Future Work” section, will help validate this hypothesis.

**Table 1. Soluble and Saturated Species for All Three Conditions Studied (bicarbonate-free samples and samples amended with 3 and 10 mM bicarbonate)**

0 mM bicarbonate		3 mM bicarbonate		10 mM bicarbonate	
Soluble	Precipitates	Soluble	Precipitates	Soluble	Precipitates
20% $\text{UO}_2\text{HPO}_4$	Hydroxylapatite	50% $\text{Ca}_2\text{UO}_2(\text{CO}_3)_3$	Hydroxylapatite	92% $\text{UO}_2(\text{CO}_3)_3^{-4}$	Hydroxylapatite
80% $\text{UO}_2\text{PO}_4^-$	Uranyl-phosphate	44% $\text{CaUO}_2(\text{CO}_3)_3^{-2}$	Uranyl-phosphate	6% $\text{CaUO}_2(\text{CO}_3)_3^{-2}$	Uranyl-phosphate
	autunite	~6% negatively charged uranyl carbonate complexes	autunite		autunite

On the other hand, the soluble species are primarily negatively charged entities in the case of bicarbonate-free samples and samples that contain 10 mM of bicarbonate; whereas in the case of samples amended with 3 mM of bicarbonate, the negatively charged and the neutral U(VI) complexes are almost 50-50%. It has been suggested in literature that negatively charged uranyl complexes are less bioavailable to the cells and the least readily reducible fraction, mostly due to electrostatic repulsions between negatively charged uranyl complexes and the bacterial cell surface (Belli et al., 2015; Sheng & Fein, 2014a). This scenario provides an additional potential explanation for the absence of bioreduction, especially in the case of bicarbonate-free samples and samples amended with 10 mM of bicarbonate, where the majority of uranyl complexes are negatively charged. On the other hand, the point of zero charge (pzc) of autunite is 5-6 (Wellman et al., 2007), which makes the net surface charge of autunite at pH 7.5 negative. Hence, one would expect electrostatic repulsion between negatively charged bacterial surfaces and the autunite surface. Bacteria were detected on the surface of autunite in the samples amended with 3 and 10 mM bicarbonate, implying that under phosphorus-limiting conditions, bacteria may overcome the electrostatic repulsion and liberate P from uranyl mineral phases to meet metabolic needs. It is not clear though to what

degree this takes place, since the amount of bacteria detected on the surface was not very high.

Although uranyl phosphates are considered to be sinks of uranium and therefore strong candidates for remediation strategies (Beazley et al., 2007), the experimental findings demonstrate their liability in the presence of bacteria.

## **Future Work**

Batch experiments that will replicate the exact conditions (U, Ca and P concentrations along with three different bicarbonate concentrations) before inoculation with bacteria in the absence of autunite (mineral-free) will take place over the same duration. The objective of this experiment will be to test the hypothesis that there are potentially two antagonistic mechanisms with similar kinetic rates are taking place. The formation of secondary minerals and bioreduction are removing U, Ca and P from the aqueous phase, while autunite dissolution is re-introducing those elements in the aqueous phase, resulting in an apparent equilibrium of those elements in the supernatant. In the proposed experiment, the decrease in the elemental concentration in the aqueous phase will signify the existence of the two antagonistic mechanisms (since there will be no autunite dissolution); whereas, if all concentrations remain the same, this will imply that the formation of secondary minerals takes place to a very limited degree and that the driving force behind the apparent equilibrium is the mineral dissolution.

## **Acknowledgement**

Funding for this research was provided by U.S. DOE cooperative agreement number DE-EM0000598. SEM/EDS analyses were conducted at FIU FCAEM facilities.

## **References**

- Bachmaf, S., Planer-Friedrich, B., Merkel, B.J. 2008. Effect of sulfate, carbonate, and phosphate on the uranium(VI) sorption behavior onto bentonite. *Radiochimica Acta*, 96(359-366).
- Barlett, M. 2014. Uranium reduction and microbial community development in response to stimulation with different electron donors.
- Beazley, M.J., Martinez, R.J., Sobecky, P.A., Webb, S.M., Taillefert, M. 2007. Uranium Biomineralization as a Result of Bacterial Phosphatase Activity: Insights from Bacterial Isolates from a Contaminated Subsurface. *Environmental Science & Technology*, 41(16), 5701-5707.
- Belli, K.M., DiChristina, T.J., Van Cappellen, P., Taillefert, M. 2015. Effects of aqueous uranyl speciation on the kinetics of microbial uranium reduction. *Geochimica et Cosmochimica Acta*, 157, 109-124.
- Bencheikh-Latmani, R., Leckie, J.O. 2003. Association of uranyl with the cell wall of *Pseudomonas fluorescens* inhibits metabolism. *Geochimica et Cosmochimica Acta*, 67(21), 4057-4066.

- Bernhard, G., Geipel, G., Reich, T., Brendler, V., Amayri, S., Nitsche, H. 2001. Uranyl(VI) carbonate complex formation: Validation of the  $\text{Ca}_2\text{UO}_2(\text{CO}_3)_3(\text{aq.})$  species. in: *Radiochimica Acta International journal for chemical aspects of nuclear science and technology*, Vol. 89, pp. 511.
- Braet, F., De Zanger, R., Wisse, E. 1997. Drying cells for SEM, AFM and TEM by hexamethyldisilazane: a study on hepatic endothelial cells. *Journal of Microscopy*, 186(1), 84-87.
- Brooks, S.C., Fredrickson, J.K., Carroll, S.L., Kennedy, D.W., Zachara, J.M., Plymale, A.E., Kelly, S.D., Kemner, K.M., Fendorf, S. 2003. Inhibition of Bacterial U(VI) Reduction by Calcium. *Environmental Science & Technology*, 37(9), 1850-1858.
- Claessens, J., van Lith, Y., Laverman, A.M., Van Cappellen, P. 2006. Acid–base activity of live bacteria: Implications for quantifying cell wall charge. *Geochimica et Cosmochimica Acta*, 70(2), 267-276.
- Donlan, R.M. 2002. Biofilms: Microbial Life on Surfaces. in: *Emerg Infect Dis*, Vol. 8.
- Ejnik, J.W., Hamilton, M.M., Adams, P.R., Carmichael, A.J. 2000. Optimal sample preparation conditions for the determination of uranium in biological samples by kinetic phosphorescence analysis (KPA). *Journal of Pharmaceutical and Biomedical Analysis*, 24(2), 227-235.
- Gudavalli, R.K.P., Katsenovich, Y.P., Wellman, D.M., Idarraga, M., Lagos, L.E., Tansel, B. 2013. Comparison of the kinetic rate law parameters for the dissolution of natural and synthetic autunite in the presence of aqueous bicarbonate ions. *Chemical Geology*, 351, 299-309.
- Hazrin-Chong, N.H., Manefield, M. 2012. An alternative SEM drying method using hexamethyldisilazane (HMDS) for microbial cell attachment studies on sub-bituminous coal. *Journal of Microbiological Methods*, 90(2), 96-99.
- Katsenovich, Y., Carvajal, D., Guduru, R., Lagos, L., Li, C.-Z. 2013. Assessment of the Resistance to Uranium (VI) Exposure by *Arthrobacter* sp. Isolated from Hanford Site Soil. *Geomicrobiology Journal*, 30(2), 120-130.
- Katsenovich, Y.P., Carvajal, D.A., Wellman, D.M., Lagos, L.E. 2012. Enhanced U(VI) release from autunite mineral by aerobic *Arthrobacter* sp. in the presence of aqueous bicarbonate. *Chemical Geology*, 308–309, 1-9.
- Khemiri, A., Carrière, M., Bremond, N., Mlouka, M., Coquet, L., Llorens, I., Chapon, V., Jouenne, T., Cosette, P., and C. Berthomieu 2014. *Escherichia coli* Response to Uranyl Exposure at Low pH and Associated Protein Regulations. *PLoS One*. 9(2): e89863.
- Langmuir, D. 1978. Uranium solution- mineral equilibria at low temperatures with application to sedimentary ore deposits. *Geochimica et Cosmochimica Acta*, **42**, 547-569.
- Lin, H., Bennett, G.N., San, K.-Y. 2005. Chemostat culture characterization of *Escherichia coli* mutant strains metabolically engineered for aerobic succinate production: A study of

- the modified metabolic network based on metabolite profile, enzyme activity, and gene expression profile. *Metabolic Engineering*, **7**(5–6), 337-352.
- Lin, X., Kennedy, D., Peacock, A., McKinley, J., Resch, C.T., Fredrickson, J., Konopka, A. 2012. Distribution of Microbial Biomass and Potential for Anaerobic Respiration in Hanford Site 300 Area Subsurface Sediment. *Applied and Environmental Microbiology*, **78**(3), 759-767.
- Marshall, M., Plymale, A., Kennedy, D., Shi, L., Wang, Z., Reed, S., Dohnalkova, A., Simonson, C., Liu, C., Saffarini, D., Romine, M., Zachara, J., Beliaev, A., Fredrickson, J. 2008. Hydrogenase- and outer membrane c-type cytochrome-facilitated reduction of technetium(VII) by *Shewanella oneidensis* MR-1. *Environmental Microbiology*, **10**(1), 125-136.
- McLean, J.S., Pinchuk, G.E., Geydebrekht, O.V., Bilskis, C.L., Zakrajsek, B.A., Hill, E.A., Saffarini, D.A., Romine, M.F., Gorby, Y.A., Fredrickson, J.K., Beliaev, A.S. 2008. Oxygen-dependent autoaggregation in *Shewanella oneidensis* MR-1. *Environmental Microbiology*, **10**(7), 1861-1876.
- Meshulam-Simon, G., Behrens, S., Choo, A.D., Spormann, A.M. 2007. Hydrogen Metabolism in *Shewanella oneidensis* MR-1. *Applied and Environmental Microbiology*, **73**(4), 1153-1165.
- Pinchuk, G.E., Geydebrekht, O.V., Hill, E.A., Reed, J.L., Konopka, A.E., Beliaev, A.S., Fredrickson, J.K. 2011. Pyruvate and Lactate Metabolism by *Shewanella oneidensis* MR-1 under Fermentation, Oxygen Limitation, and Fumarate Respiration Conditions. *Applied and Environmental Microbiology*, **77**(23), 8234-8240.
- Sánchez, A.M., Bennett, G.N., San, K.-Y. 2005. Novel pathway engineering design of the anaerobic central metabolic pathway in *Escherichia coli* to increase succinate yield and productivity. *Metabolic Engineering*, **7**(3), 229-239.
- Sheng, L., Fein, J.B. 2013. Uranium adsorption by *Shewanella oneidensis* MR-1 as a function of dissolved inorganic carbon concentration. *Chemical Geology*, **358**, 15-22.
- Sheng, L., Fein, J.B. 2014a. Uranium Reduction by *Shewanella oneidensis* MR-1 as a Function of  $\text{NaHCO}_3$  Concentration: Surface Complexation Control of Reduction Kinetics. *Environmental Science & Technology*, **48**(7), 3768-3775.
- Sheng, L., Fein, J.B. 2014b. Uranium reduction by *Shewanella oneidensis* MR-1 as a function of  $\text{NaHCO}_3$  concentration: surface complexation control of reduction kinetics. *Environmental Science and Technology*, **1**(48), 3768-3775.
- Smeaton, C.M., Weisener, C.G., Burns, P.C., Fryer, B.J., Fowle, D.A. 2008. Bacterially enhanced dissolution of meta-autunite. *American mineralogist*, **93**, 1858-1864.
- Tang, Y.J., Laidlaw, D., Gani, K., Keasling, J.D. 2006. Evaluation of the effects of various culture conditions on Cr(VI) reduction by *Shewanella oneidensis* MR-1 in a novel high-throughput mini-bioreactor. *Biotechnology and Bioengineering*, **95**(1), 176-184.

- Thormann, K.M., Saville, R.M., Shukla, S., Pelletier, D.A., Spormann, A.M. 2004. Initial Phases of Biofilm Formation in *Shewanella oneidensis* MR-1. *Journal of Bacteriology*, **186**(23), 8096-8104.
- Wellman, D.M., Gunderson, K.M., Icenhower, J.P., Forrester, S.W. 2007. Dissolution kinetics of synthetic and natural meta-autunite minerals,  $X_3-n(n)+ [(UO_2)(PO_4)]_2 \cdot xH_2O$ , under acidic conditions. *Geochemistry, Geophysics, Geosystems*, **8**(11), n/a-n/a.
- Wu, C., Cheng, Y.-Y., Yin, H., Song, X.-N., Li, W.-W., Zhou, X.-X., Zhao, L.-P., Tian, L.-J., Han, J.-C., Yu, H.-Q. 2013. Oxygen promotes biofilm formation of *Shewanella putrefaciens* CN32 through a diguanylate cyclase and an adhesin. *Scientific Reports*, **3**, 1945.